

Mars Observer Trajectory and Orbit Control

C. A. Halsell* and W. E. Bollman†

Jet Propulsion Laboratory, California Institute of Technology, Pasadena, California 91109

The Mars Observer mission will study Mars from a low-altitude orbit. During interplanetary cruise, propulsive maneuvers are required to ensure capture, with a secondary constraint to satisfy limits on the probability of impact with Mars. After capture, the spacecraft will be brought to a near-circular mapping orbit through a series of maneuvers. Mapping orbit maneuvers will be performed in order to follow a predetermined set of ground tracks and to maintain orbit altitude. This will allow accurate spacecraft command sequence generation and aid science planning throughout the mapping phase. Specific orbit control plans for the open and close of the launch period have been developed to meet these needs. This paper describes the control capabilities and the associated expected velocity changes for the mission.

Nomenclature

a	= orbit semimajor axis, km
e	= orbit eccentricity
I	= orbit inclination, deg
R_A	= radius of apoapsis, km
R_P	= radius of periapsis, km
ΔV	= velocity change, m/s
ΔV_{99}	= 99th percentile velocity change, m/s
μ	= statistical mean
σ	= standard deviation
ω	= orbit argument of periapsis, deg
Ω	= longitude of the orbit ascending node, deg

Introduction

DURING the course of the Mars Observer mission, maneuvers changing the velocity of the spacecraft will be implemented to achieve the desired trajectory (attitude control maneuvers are also necessary but are not discussed here). These must be accomplished within a limited ΔV budget and to a high degree of certainty. Detailed mission studies have been performed for the open and close of the launch window from Sept. 16, 1992 to Oct. 5, 1992.

The overall maneuver strategy for Mars Observer is to deliver the spacecraft to the near-circular mapping orbit accurately and with minimum propellant usage. Once achieved, the mapping orbit will be maintained within prescribed limits, correcting for planetary gravitational anomalies and atmospheric drag. These goals must be met while conforming to constraints on probability of impact with Mars and avoiding the dangerous exposure of certain scientific components to direct sunlight. This paper describes the maneuvers needed to accomplish the mission and describes strategies to operate within these constraints.

Mission Trajectory Description

The mission may be divided into launch, cruise, orbit insertion, and mapping phases. Launch and injection occur from Sept. 16, 1992 to Oct. 5, 1992, using a Titan III/ Transfer

Orbit Stage (TOS) combination. A maneuver time line is shown in Fig. 1. The cruise phase extends from injection into the Earth-Mars trajectory until Mars encounter. Trajectory correction maneuvers (TCMs) will correct for injection, maneuver execution, and orbit determination (OD) errors and will meet planetary protection requirements. For some launch dates, a maneuver is also necessary to optimize the trajectory.

The second phase of the mission is the orbit insertion phase. The Mars orbit insertion (MOI) maneuver results in an three-day elliptical capture orbit. This is followed by a sequence of deterministic and statistical maneuvers designed to bring the spacecraft to the mapping orbit by Nov. 22, 1993. Because of a solar conjunction on Dec. 27, 1993, a spacecraft command moratorium exists from Dec. 16, 1993 to Jan. 7, 1994. No maneuvers are scheduled during this time. After conjunction, a trim maneuver may be needed to bring the mapping orbit to the correct eccentricity.

The mapping phase begins 10 days after the mapping orbit has been established and lasts for one Mars year (687 Earth days). The orbit has a period of 1.96 h and is nearly circular. Additionally, it should be frozen; that is, the orbit elements must be chosen such that planetary oblateness effects will maintain a nearly constant orbit eccentricity and argument of periapsis. The sunlit descending node will return to approximately the same longitude every seven days. In practice, this node longitude will move gradually to the east, resulting at the end of the mission in ground tracks spaced only 3.1 km apart at the equator.

During mapping, the orbit will be perturbed by gravity field anomalies and atmospheric drag forces. A longitude grid control strategy (LGC) will be used to simplify mission operations. The longitude grid is a set of ground tracks and equator crossing times for the entire mapping phase. Orbital trim maneuvers (OTMs) will occur every two weeks, if necessary, to keep to the grid and maintain the frozen orbit. Because the expected magnitude of these maneuvers is close to the minimum thruster capabilities, the execution error of the maneuvers is a significant error source.

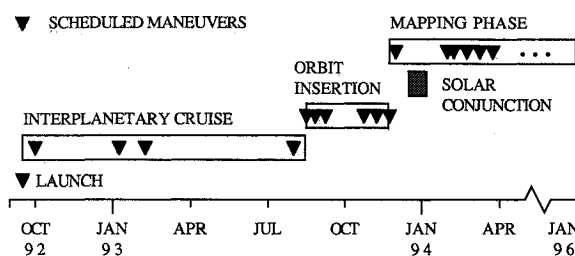


Fig. 1 Mars Observer mission time line.

Received Dec. 11, 1989; revision received May 3, 1991; accepted for publication May 4, 1991. Copyright © 1991 by the American Institute of Aeronautics and Astronautics, Inc. The U.S. Government has a royalty-free license to exercise all rights under the copyright claimed herein for Governmental purposes. All other rights are reserved by the copyright owner.

*Member of the Technical Staff, Navigation Systems Section. Member AIAA.

†Technical Group Supervisor, Navigation Systems Section.

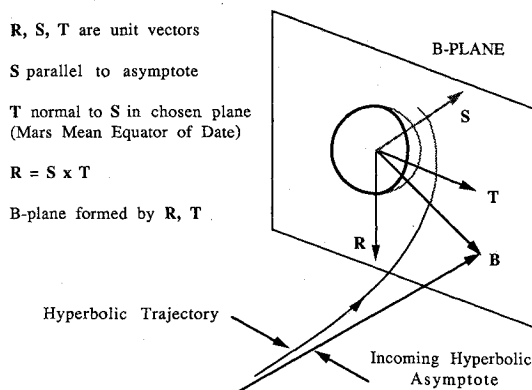


Fig. 2 B-plane coordinate system.

Spacecraft Thruster Characteristics

The Mars Observer spacecraft will be equipped with bipropellant and hydrazine (monopropellant) thrusters. A bipropellant system of four 490-N engines and four 22-N engines will be used for cruise maneuvers. Hydrazine thrusters must be used once the spacecraft is in mapping configuration to avoid contamination of the science instruments. The hydrazine system consists of eight 4.4-N engines and four 0.88-N engines.

The spacecraft contract limits the fixed magnitude error to 0.05 m/s (3 σ), and the proportional magnitude error to 2% (3 σ). Side velocity errors (in effect, pointing errors) may not exceed a fixed value of 0.01 m/s (3 σ) and a proportional value of 2.5% (3 σ). However, since no calibration maneuver will be performed, the side velocity errors will be larger for the first use of each bipropellant engine group.¹ For the expected range of velocity changes, the 490-N engine group expected side velocity error is fixed at 3.3 m/s (3 σ). The side velocity errors for the 22-N group are 16% (3 σ) for $0 < \Delta V \leq 5$ m/s, and 0.8 m/s (3 σ) for $\Delta V > 5$ m/s.

Monte Carlo Techniques

Monte Carlo modeling of the trajectory and its associated errors allows relatively simple analysis of a complicated system. For the interplanetary phase, maneuvers are treated as perturbations to a linearized two-body heliocentric trajectory.² Errors in the knowledge of the spacecraft state (i.e., orbit determination errors³) are included, causing errors in the desired velocity change. Maneuver execution errors further degrade the ΔV , producing errors at encounter. In this way, the mission can be flown multiple times and the results recorded.

For the cruise, each sample of the simulation follows these steps.

1) Perturb the nominal trajectory at injection by sampling the TOS injection error.

2) For each of four trajectory corrections, a) propagate the actual state from the previous maneuver; b) perturb this true state by sampling the orbit determination errors, creating an estimate of the state; c) based on this estimate, determine the velocity change that will correct the predicted error with respect to the next aim point; d) corrupt this desired velocity change with maneuver execution errors; and e) apply this actual velocity change, based on an incorrect state estimate, to the true state and the state estimate.

3) Propagate the state after the final trajectory correction to encounter and record the total velocity change for cruise, the state at encounter, and other parameters.

This simple example is meant only to illustrate the process. In fact, the simulation continues through the orbit insertion phase in a similar manner, calculating the ΔV for each maneuver to eventually reach the mapping orbit. Typically, 1000 samples are used, although more may be used for greater precision in high-percentile values (ΔV_{99} , for instance).

Planetary Protection Requirements

NASA has established requirements to avoid contamination of Mars by terrestrial organisms.⁴ They dominate the choice of interplanetary aim points. The applicable requirements are 1) the probability of impact of the spacecraft on Mars throughout the mission must be $\leq 10^{-4}$, and 2) the probability of impact of the launch vehicle on Mars must be $\leq 10^{-5}$. This section describes how these requirements are met.

B-Plane Coordinate System

Conditions at encounter are described in the B-plane coordinate system (Fig. 2). The B plane, formed by the R and T axes, is perpendicular to the incoming hyperbolic asymptote at Mars. Aim points are described by the projection of B onto R and T, i.e., $B \cdot R$ and $B \cdot T$. Keep in mind that the aim points do not describe the location of the spacecraft, but of the asymptote at encounter. The ΔV needed for a maneuver is calculated from

$$\Delta V = K^{-1} \Delta B \quad (1)$$

where K is the partial of $B \cdot R$, $B \cdot T$, and linearized time of flight with respect to spacecraft velocity.

Impact Probabilities

In this analysis, the 10^{-4} impact requirement for the spacecraft is interpreted: 1) the probability p_i that the spacecraft is on an impact trajectory must be $\leq 10^{-2}$, and 2) the probability p_f that the next maneuver fails to occur must be $\leq 10^{-2}$. This may be expressed as

$$P(\text{impact}) = p_i p_f \quad (2)$$

In the B plane, there is an impact radius B_{IR} that limits the closest possible approach to the planet.⁵ Any closer approach results in impact. This impact radius is described by

$$B_{IR} = r_0 \sqrt{\frac{2GM}{r_0 V_\infty^2} + 1} \quad (3)$$

where r_0 and GM are the radius and gravitational constant of Mars, respectively, and V_∞ is the trajectory hyperbolic excess velocity. The impact probability p_i is the integral of the B plane dispersion ellipse (with mean B_0 and covariance matrix Σ) over the impact radius,

$$p_i = \frac{1}{2\pi |\Sigma|^{1/2}} \iint_{|B| \leq B_{IR}} \exp[-\frac{1}{2}(B-B_0)^T \Sigma^{-1} (B-B_0)] dB \quad (4)$$

Some missions have included a term in Eq. (2) to allow for the recovery from a spacecraft failure.^{5,6} For planning purposes, we assume no such recovery is possible (erring on the side of conservatism).

Table 1 Mars Observer interplanetary ΔV

Maneuver	Design ΔV , m/s	$\mu \Delta V$, m/s	$\sigma \Delta V$, m/s	ΔV_{99} , m/s
Sept. 16, 1992, launch date				
TCM-1	0	19.7	18.1	74.8
TCM-2	80.9	77.9	5.3	88.7
TCM-3	1.9	2.1	0.5	3.4
TCM-4	1.7	2.3	0.9	5.6
Cruise total	84.5	102.0	14.1	144.8
Oct. 5, 1992, launch date				
TCM-1	3.2	22.7	16.8	72.6
TCM-2	4.9	6.2	3.0	14.2
TCM-3	0.4	0.5	0.2	0.9
TCM-4	0.01	0.7	0.4	1.7
Cruise total	8.5	30.0	17.6	83.3

Interplanetary Propulsive Maneuver Analysis

The maneuver analysis task for the cruise phase of the mission involves determination of the timing and magnitudes of the injection and the TCMs. For launch dates from Sept. 16 to Sept. 19, 1992, TCM-2 results in a slight plane change and is used to optimize the interplanetary trajectory. This broken plane maneuver takes place on a given date and has an effect on the planetary protection strategy.

Uncertainties about the spacecraft position and velocity improve during the mission as tracking data are analyzed. Therefore, each TCM will reduce the expected Mars encounter distance to satisfy these restrictions.

Injection Aim-Point Biasing

Recall that the TOS upper stage must have $\leq 10^{-5}$ probability of impact with Mars. No Mars avoidance maneuver will be performed by the TOS after spacecraft separation. Instead, the requirement will be met by changing the aim point for the spacecraft injection (aim-point biasing). Aim-point biasing is performed for all cruise maneuvers that exceed the required probability of impact. Some deterministic maneuvers have satisfactory impact probabilities and need not be biased.

For all launch dates, the $1\text{-}\sigma$ injection dispersion ellipse in the B plane is approximately 1.9×10^6 km by 4.0×10^4 km. The nominal spacecraft encounter aim point is $B \cdot R = -8220$ km, $B \cdot T = -416$ km. For the Sept. 16, 1992, launch, the broken plane maneuver (TCM-2) moves the aim point by approximately 2.8×10^6 km. At injection there is virtually zero probability of impact. For the Oct. 5, 1992, launch, the aim point will be biased by approximately 7.5×10^5 km to meet the 10^{-5} impact probability. Some intervening launch dates have been studied, but these two dates represent the expected launch date and highest fuel requirement, respectively.

Interplanetary Maneuver Placement and ΔV

Interplanetary maneuvers are needed to keep the spacecraft on course and to satisfy the planetary protection requirements. The maneuver strategy for selecting interplanetary aim points is to minimize the deterministic ΔV . To pick the aim points, a probability of impact contour in the B plane is produced for each maneuver (and for injection if necessary). The ΔV needed to move between points on the contours is found from Eq. (1), and the set of aim points that minimizes the sum of the deterministic ΔV for each maneuver is chosen.

The first TCM is scheduled 15 days after injection, primarily to clean up the injection errors. This is the earliest possible date for the maneuver given the tasks that must be performed by the various mission teams. A backup date for this maneu-

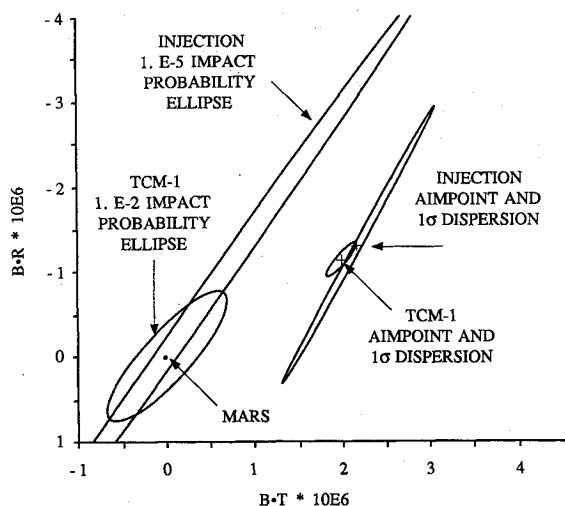


Fig. 3 September 16, 1992, launch date: injection and TCM-1 aim points.

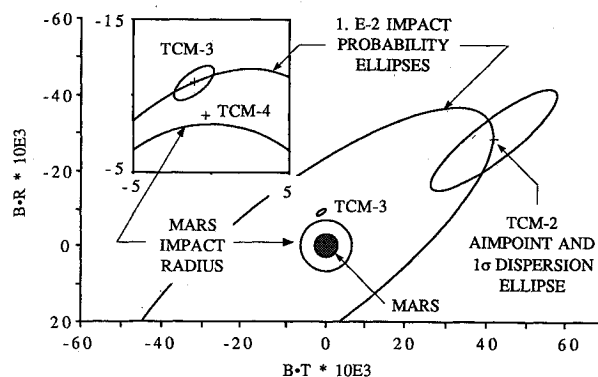


Fig. 4 September 16, 1992, launch date: TCM-2 through TCM-4 aim points.

ver has been set 15 days later, at 30 days after injection. Trajectories that launch between Sept. 16 and Sept. 19, 1992, require broken plane maneuvers approximately 114 days after launch. To simplify mission operations, the date for TCM-2 has been set on Jan. 8, 1993, for all launch dates. For the first launch date, this broken plane component is sufficient to satisfy planetary protection requirements as stated earlier; where this component is small, additional biasing may be required. In addition, two-impulse optimization will be performed between TCM-1 and TCM-2 to reduce the sum of the ΔV .

TCM-3 corrects for the errors of the previous maneuver and reduces the Mars encounter distance to a 10^{-2} probability of impact. Its date has been fixed on Feb. 8, 1993. TCM-4 takes place 15 days before Mars encounter to prepare for MOI.

The ΔV magnitude of each maneuver is given in Table 1 along with the total cruise ΔV . The design ΔV is the deterministic velocity change needed at each maneuver. The ΔV_{99} is the 99th percentile ΔV , sufficient to perform 99% of the expected maneuvers. This value is used for mission planning and propellant loading. For a Gaussian (normal) distribution, the 99th percentile is approximately the mean value plus 2.33 standard deviations ($\mu + 2.33 \sigma$). This is not a valid assumption for results given here since the distribution of ΔV is non-Gaussian.

The Sept. 16, 1992, launch date shows some interesting results. The magnitude of TCM-2 ranges from 82.7 m/s to 0, depending on the launch date and time. The ballistic ΔV for TCM-2 on the first launch date is 82.7 m/s. Note that both the design ΔV and the mean ΔV in Table 1 are lower than this value. The design ΔV is lower because the aim point for TCM-2 is not the final aim point; additional corrections are made at TCM-2 and TCM-3. This has the effect of increasing the total design ΔV over the optimal value—the cruise total is 84.5 m/s. The mean TCM-2 ΔV is lowered by the optimization with TCM-1.

Note also that the design ΔV for TCM-1 on this date is zero because the optimal maneuver time is at TCM-2. Once injection errors are introduced, TCM-1 is needed.

Figures 3 and 4 illustrate the cruise aim points for the Sept. 16, 1992, launch date. In Fig. 3, the injection and TCM-1 B -plane aim points are shown, along with the $1\text{-}\sigma$ dispersions and appropriate probability of impact ellipses (10^{-5} and 10^{-2}). Figure 4 shows the same information for the subsequent TCMs. Note the gradual move of the aim points to the final value (at TCM-4) and the reduction of the size of the dispersion ellipses.

Mars Orbit Insertion Phase Analysis

It is not desirable to maneuver directly to the mapping orbit from interplanetary cruise. Three intermediate orbits with periods of 72, 24, and 4.2 h will be employed. This design allows the orbit to move to the desired 2 p.m. mapping orientation, reduces the cumulative finite burn gravity losses, and results in

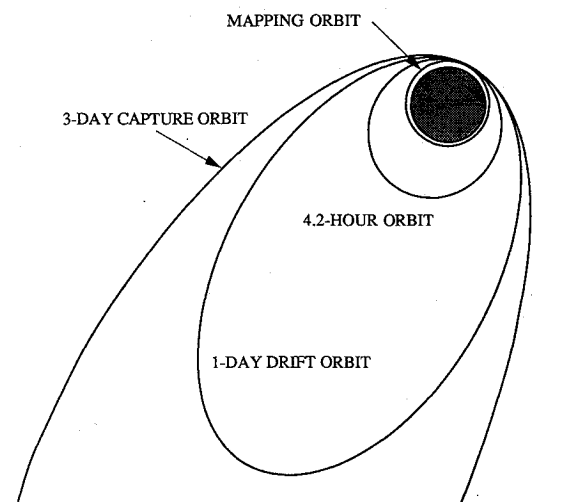


Fig. 5 Mars orbit insertion phase.

low orbit element errors once the spacecraft is in near-circular orbit. The orbits in this phase are illustrated in Fig. 5.

The MOI maneuver results in a three-day capture orbit with periapsis of 3950 km (553-km altitude). Periapsis height is lowered at the next burn, elliptical correction maneuver 1 (ECM-1). ECM-2 establishes the one-day drift orbit. This orbit is less susceptible to the perturbations that keep the mapping orbit Sun synchronous and drifts to the desired 2 p.m. mapping orientation from its initial 5 p.m. orientation over a period of 43–63 days. ECM-3 will trim inclination and periapsis radius in the drift orbit.

Mapping orbit is achieved by two transfer to low orbit maneuvers, TLO-1 and TLO-2. These maneuvers take place near periapsis to lower apoapsis and rotate the periapsis to the south pole. Ideally, these would result in a mapping orbit. However, residual orbit element errors after TLO-2 might cause the orbit to be nonfrozen, and so the orbital correction maneuver 1 (OCM-1) is necessary before the gravity calibration period may begin. Gravity calibration is needed to refine present models of the Mars gravity field and to calculate the correct eccentricity for a frozen orbit. The nominal mapping orbit has an index altitude of 378.1 km [defined as orbit semimajor axis—Mars equatorial radius (3397.2 km)]. The period is 1.96 h and periapsis is above the south pole.

Establishment of Mapping Orbit

The MOI burn will use two of the four 490-N bipropellant engines; the remaining two will serve as backups. It is planned to be a constant pitch-rate, in-plane maneuver. Depending on the launch date, the true anomaly at ignition will range from -48° to -54° , moving through an arc of 89° – 100° . The burn duration is from 1440 to 1674 s. In the Monte Carlo analysis, MOI is the only maneuver simulated as nonimpulsive. However, TLO-1 and TLO-2 are also long-duration maneuvers with appreciable finite burn gravity losses.⁷ The total gravity losses during the orbit insertion phase range from 38 to 47 m/s.

The necessary ΔV for each maneuver is summarized in Table 2. Only the MOI and ECM-1 ΔV differ by launch date, and so these are presented separately. The reason for this similarity between launch dates is that the errors due to MOI are primarily apoapsis height errors, which are corrected at ECM-1. ECM-3 and OCM-1 are clean-up maneuvers and, therefore, have zero deterministic ΔV . Orbit determination errors⁵ were included in the Monte Carlo program.

Initial Mapping Orbit Control

The orbit after OCM-1 may not be changed for five weeks, because of solar conjunction and the associated command

Table 2 Mars Observer orbit insertion phase ΔV

Maneuver	Design ΔV , m/s	$\mu \Delta V$, m/s	$\sigma \Delta V$, m/s	ΔV_{99} , m/s
MOI				
9/16/92 launch date	670	669	5.3	682
10/5/92 launch date	762	762	6.2	777
ECM-1				
9/16/92 launch date	4.0	6.0	2.6	14.2
10/5/92 launch date	4.0	5.8	2.6	14.0
ECM-2	122	123	9.5	148
ECM-3	0	0.1	0.1	0.4
TLO-1	549	549	3.8	558
TLO-2	622	623	5.9	637
OCM-1	0	5.9	3.0	14.2

Table 3 Control on initial Mars Observer mapping orbit

Orbit element	Mean value	1 σ
a , km	3775.3	0.10
e	0.0072	0.0002
I , deg	92.87	0.04
Ω , deg	38.34	0.87
ω , deg	-90.0	3.3
R_p , km	3748.0	0.6

moratorium. Clearly, orbit errors must be small for this to be a safe strategy. Orbit errors in combination with planetary gravity field errors or high atmospheric drag might cause the spacecraft orbit to be unstable during this period. The orbit insertion maneuver plan delivers the spacecraft to mapping orbit with a high degree of accuracy, as shown in Table 3.

Mapping Phase Maneuver Analysis

The orbital elements of the mapping orbit will deviate from the nominal values because of perturbations due to gravity field anomalies, maneuver execution errors, and Mars atmospheric drag. OTMs will be necessary to adjust the orbit period to maintain the repeating ground track pattern and to keep the orbit eccentricity and argument of periapsis relatively constant (i.e., a frozen orbit). The LGC strategy will control the semimajor axis within 0.2 km (3σ) of its nominal value.

As noted, the hydrazine thruster system will be used for all mapping phase maneuvers. The maneuver plan is constrained by the 50-mm/s (3σ) fixed magnitude execution error of these thrusters, which places a lower bound on the magnitude of an achievable maneuver.

Mapping Phase Startup

The targeted frozen orbit will not be precisely frozen because of gravity field errors. After processing data from the seven-day gravity calibration period, the gravity field will be refined sufficiently to establish the proper target eccentricity. The final eccentricity of the frozen mapping orbit may differ from the current nominal value of 0.007 by ± 0.006 (3σ). OTM-1 will bring the orbit to this eccentricity on Jan. 28, 1994. Its mean expected magnitude is 5.3 m/s with a 3σ high of 20 m/s.

Nominal Mapping Strategy

The Mars Observer frozen mapping orbit provides an approximate 58.6-km eastward walk between adjacent ground tracks at the Mars equator. These adjacent ground tracks occur every 88 revs/7 Mars days, i.e., the equator crossing at orbit 89 will be 58.6 km to the east of orbit 1.

The project adopted LGC in order to solve an orbit prediction problem in sequence planning. The grid design is a set of evenly spaced longitudes and associated equator crossing times based on the nominal mapping orbit ground tracks. OTMs are planned every two weeks, and each maneuver will target to reach the grid in two weeks. For example, OTM-2 on

Feb. 7, 1994, will be the first LGC maneuver and will target to the desired longitude and time at OTM-3, two weeks later. Thus, actual grid control will begin on Feb. 21, 1993. The maneuvers will be performed either along or opposite the velocity vector at periapsis. Sometimes the maneuver may be performed at apoapsis to assist in controlling the eccentricity. Additionally, some maneuvers (such as OTM-2) will be used for inclination correction when necessary.

The ground track repeat and walk interval depend on the orbit period, and so they are quite sensitive to errors in the semimajor axis. For each 0.2-km change in the mean semimajor axis, the walk interval between adjacent ground tracks changes by about 11.8 km. As noted, dispersions in the semimajor axis can be caused by atmospheric drag and by the Mars gravity field. When a trim maneuver is executed to alter or correct the orbital elements, maneuver execution errors perpetuate a small error in the semimajor axis. The ability to maintain the semimajor axis depends on the execution accuracy and on the OD capability. The accuracy of the OTM magnitude (50 mm/s, 3σ) corresponds to 0.11-km semimajor axis control (3σ). The OD capability appears to be a fraction of this value after gravity calibration.

Mars Atmospheric Drag Variation

Atmospheric drag affects the ground track walk interval by reducing the orbit semimajor axis. Short-term and long-term density variations result from a variety of sources. The long-term density is believed to be well understood; however, uncertainty in the short-term density is high. The F10.7-cm solar flux level is a major error source in the atmosphere model, as is the presence of dust storms on the surface. Both these effects peak near Mars perihelion. At Mars perihelion, the 50th percentile subsolar-point density for the 378.1-km mapping orbit⁸ is approximately 3.5×10^{-14} kg/m³; the 3σ high density is near 58.5×10^{-14} kg/m³. Day-to-day variations of solar flux were not included in the short-term density prediction errors. There is reason to suspect that these solar flux variations may cause daily density variations. If this is the case, the equator crossing errors may be 2-5 times larger than shown here once this error source is included.

Longitude Grid Control

These uncertainties limit the orbit prediction capability. Studies have shown that atmospheric density can be determined in flight to an accuracy of 7.6×10^{-14} kg/m³ (1σ) and predicted ahead with the same uncertainty for three weeks.⁵

It is possible to estimate grid errors in case of higher atmospheric errors. Figure 6 shows the 99th percentile equator crossing grid accuracy at Mars perihelion plotted as a function of the 1σ in-flight density determination. The grid accuracy is given in kilometers at the equator rather than degrees. Values

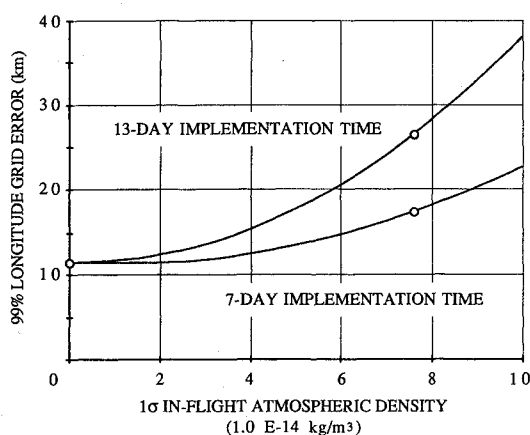


Fig. 6 99% longitude grid errors.

Table 4 Mars Observer baseline total ΔV budget

Subphase	Sept. 16, 1992, launch date		Oct. 5, 1992, launch date	
	Estimate, m/s	Allocation, m/s	Estimate, m/s	Allocation, m/s
Bipropellant ΔV				
TCM ΔV_{99}	62	60	83	70
Broken plane ΔV	83 ^a	101 ^b	0 ^a	0
MOI	670 ^a	664	762 ^a	766
Reach mapping	1335	1365	1334	1365
Finite burn losses	38	48	47	48
Mission total	2164 ^c	2238	2207 ^c	2249
Hydrazine ΔV				
Maneuver orbit trims	26	45	26	45

are given for two possible maneuver design and implementation times (7 and 13 days) and represent bounds on the expected error. With seven days of available OD and the expected in-flight density error, the mean equatorial grid error is about 5.2 km. The 99th percentile value shown in the figure is 17.2 km. In terms of an equator crossing timing error, the capability is about 21 s (mean error), or 70 s (99%). The ΔV_{99} for each of these maneuvers is approximately 130 mm/s. Equator crossing accuracy will be improved at aphelion, where the atmospheric density and its variation is lower.

ΔV for the Mapping Phase

The total ΔV for the mapping phase is a combination of the ΔV needed to compensate for atmospheric drag, that needed to correct for gravity anomalies and maneuver execution errors, and the maneuver to initiate LGC. The average 3σ high atmospheric density throughout the mapping phase is about 2.2×10^{-14} kg/m³, equivalent to a 3σ high ΔV of about 3 m/s (assuming a spacecraft ballistic coefficient of 29 kg/m²).

The total ΔV for the mapping phase will be about 26 m/s (3σ). This includes the OTM-1 orbit refreeze maneuver and corrections for atmospheric drag, gravity anomalies, and inclination. It also includes an additional three months of mapping orbit operation in support of the Mars Balloon Relay for the Soviet Mars 1994 mission. The current ΔV allocation for the mapping phase for all OTMs is 45 m/s, which should be enough to correct for extreme dispersions in the orbit due to atmospheric drag and gravity anomalies and to allow longitude grid control to be implemented.

Total Mission ΔV

The total ΔV needed for propulsive maneuvers is summarized in Table 4. The total bipropellant ΔV_{99} is the total for the cruise and orbit insertion phases. Although the allocation for some subphases is marginally exceeded, it is this total ΔV that must be met. This estimated ΔV is less than the allocation, which is used to predict required propellant loading on the spacecraft.

The total hydrazine ΔV for the mapping phase of the mission is the 3σ high value, rather than the 99th percentile high. This adds more conservatism in the area with the most uncertainties and unknowns, i.e., atmospheric drag and gravity perturbations on the orbit.

Conclusions

The trajectory of the Mars Observer spacecraft and restrictions on the interplanetary trajectory require considerable ΔV , but the expected velocity change is within the allocation. Additionally, the mapping orbit strategy calls for precise mapping and good long-term knowledge of the atmospheric density. The present work indicates that the longitude errors are acceptably low; however, changes in the treatment of daily solar flux variations may increase these errors. Recent evidence that

the actual execution errors for the hydrazine thrusters may decrease will probably not lower the longitude or timing errors given earlier (atmospheric density prediction errors will dominate).

Finally, some instruments (notably the Mars Observer camera and the Mars Observer laser altimeter) require pointing restrictions on the spacecraft to avoid exposure to the Sun. These and any other instrument constraints must be taken into account and alternate maneuver plans made.

Acknowledgment

The work described in this paper was performed by the Jet Propulsion Laboratory, California Institute of Technology, under a contract with NASA.

References

¹Tracy, T., "Maneuver Side-Velocity Error Requirement—Calibration Burn Considerations," General Electric Astro-Space Division,

Princeton, NJ, MO-AAC-001-184, March 1990.

²Chadwick, C., and Miller, L. J., "An Overview of the ADAM Maneuver Analysis System," AIAA Paper 83-411, Aug. 1983.

³Esposito, P. B., "Mars Observer Project Navigation Plan," Jet Propulsion Lab., California Inst. of Technology, Pasadena, CA, ID 642-312, Rev. C, June 1990.

⁴"Biological Contamination Control for Outbound and Inbound Planetary Spacecraft," NASA Management Instruction 8020.7A, May 1988.

⁵Maize, E. H., "Earth Flyby Delivery Strategies for the Galileo Mission," American Astronautical Society Paper 89-427, Aug. 1989.

⁶O'Neil, W. J., "Viking 1975 Navigation Plan, Volume II," Jet Propulsion Lab., California Inst. of Technology, Pasadena, CA, ID 612-32, May 1975.

⁷Robbins, H. M., "An Analytical Study of the Impulsive Approximation," *AIAA Journal*, Vol. 4, No. 8, 1966, pp. 1419-1423.

⁸Bass, L. E., "Density Profiles for 378.1 km MO Mapping Orbit, Using Marshall Solar Flux Model," Jet Propulsion Lab., California Inst. of Technology, Pasadena, CA, JPL IOM 312/90.2-1583, Jan. 1990.

Recommended Reading from the AIAA

Progress in Astronautics and Aeronautics Series . . . 

Spacecraft Dielectric Material Properties and Spacecraft Charging

Arthur R. Frederickson, David B. Cotts, James A. Wall and Frank L. Bouquet, editors

This book treats a confluence of the disciplines of spacecraft charging, polymer chemistry, and radiation effects to help satellite designers choose dielectrics, especially polymers, that avoid charging problems. It proposes promising conductive polymer candidates, and indicates by example and by reference to the literature how the conductivity and radiation hardness of dielectrics in general can be tested. The field of semi-insulating polymers is beginning to blossom and provides most of the current information. The book surveys a great deal of literature on existing and potential polymers proposed for noncharging spacecraft applications. Some of the difficulties of accelerated testing are discussed, and suggestions for their resolution are made. The discussion includes extensive reference to the literature on conductivity measurements.

TO ORDER: Write, Phone or FAX:

American Institute of Aeronautics and Astronautics
c/o TASCOT
9 Jay Gould Ct., P.O. Box 753, Waldorf, MD 20604
Phone (301) 645-5643, Dept. 415 • FAX (301) 843-0159

Sales Tax: CA residents, 7%; DC, 6%. For shipping and handling add \$4.75 for 1-4 books (call for rates for higher quantities). Orders under \$50.00 must be prepaid. Foreign orders must be prepaid. Please allow 4 weeks for delivery. Prices are subject to change without notice. Returns will be accepted within 15 days.

1986 96 pp., illus. Hardback
ISBN 0-930403-17-7

AIAA Members \$29.95

Nonmembers \$37.95

Order Number V-107